

Charge Density Waves in a Quantum Plasma

Zhaoyu Han,¹ Shiwei Zhang,^{2,3,*} and Xi Dai^{4,†}

¹*Department of Physics, Stanford University, Stanford, California 94305, USA*

²*Center for Computational Quantum Physics, Flatiron Institute, New York, New York 10010, USA*

³*Department of Physics, The College of William and Mary, Williamsburg, Virginia 23187, USA*

⁴*Physics Department, Hong Kong University of Science and Technology, Hong Kong, China*

(Dated: October 17, 2019)

We analyze the instability of an unpolarized uniform quantum plasma consisting of two oppositely charged fermionic components with varying mass ratios, against charge and spin density waves (CDW's and SDW's). Using density functional theory, we treat each component with the local spin density approximation and a rescaled exchange-correlation functional. Interactions between different components are treated with a mean-field approximation. In both two- and three-dimensions, we find leading unstable CDW modes in the second-order expansion of the energy functional, which would induce the transition to quantum liquid crystals. The transition point and the length of the wave-vector are computed numerically. Discontinuous ranges of the wave-vector are found for different mass ratios between the two components, indicating exotic quantum phase transitions. Phase diagrams are obtained and a scaling relation is proposed to generalize the results to two-component fermionic plasmas with any mass scale. We discuss the implications of our results and directions for further improvement in treating quantum plasmas.

PACS numbers: 52.35.-g, 64.70.Tg, 71.45.Lr

I. INTRODUCTION

Plasma, as one of the four fundamental states of matter, can be generally understood as a mixture of roaming ions, whose behavior is usually dominated by collective effects mediated by the electromagnetic force. Past studies have primarily focused on the classical or semi-quantum region, where at least one of the components is not fully treated with quantum mechanics. For example, calculations with the coupled electron-ion Monte Carlo (MC) method typically neglect ionic exchange interaction^{1,2}, and path integral MC or molecular dynamics methods often do not include a full description of quantum statistics³⁻⁸. Those simplified calculations considered not only the computational challenges and expenses of a complete treatment of full quantum effects, but also the relative rarity of situations where the plasma is dense and cold enough so that quantum effects dominate the behaviors of all component. Such systems, however, can be found in the interior of giant planets or white dwarf stars, and in the world of condensed matter physics. For example, in semiconductors, the effective particles and holes introduced by the electronic band structure could play the roles of the two different types of ions⁹⁻¹¹, for which the behavior must be understood with quantum theories. (See, e.g. Ref.¹² for case studies of equal masses.) Recently, increasing attention has focused on nuclear quantum effects¹³.

A particular kind of plasma that can be viewed as of extremely large mass ratio, the electron gas in the background of positively charged jellium, is one of the most fundamental models in many-body physics and has been extensively investigated^{14,15}. Density Functional Theory (DFT) calculations¹⁶⁻¹⁸ rely on the correlation energies of the electron gas as a foundation. Because

of both analytical and numerical challenges, the phase diagram of this model remains incomplete. The intermediate phases between the high-density limit and the opposite limit, which are the uniform liquid phase and the Wigner crystal phase respectively, are uncertain¹⁹⁻²². Quantum MC (QMC)²³⁻³⁸ calculations, which have provided the parametrization for the correlation energies to serve as the basis for most modern DFT calculations, are the most sophisticated numerical treatment. However, one can still be limited by the candidate structure or accuracy (e.g. from the fixed-node approximation²³ with the trial wave function), finite-size effects, and incommensurability with the true ground state structure. Many Hartree-Fock (HF)³⁹⁻⁴³ calculations indicate possible additional phases of magnetic and charge order, but the relevance of these predictions to the actual many-body ground state is difficult to establish because of the crude nature of the approximation.

In this paper, the quantum limit (i.e. at high density and zero temperature) of a two-component plasma is investigated at all mass ratios, by means of DFT within the framework of local spin density approximation (LSDA). Neglecting the correlation effects between the two components beyond electrostatics (Hartree), we calculate the ground-state energy as functional of their density distributions. An analysis of second-order expansion of the energy functional shows that the unpolarized uniform liquid state is unstable against CDWs with infinitesimal amplitudes at certain densities, which could eventually lead to the formation of (smectic) quantum liquid crystals⁴⁴⁻⁴⁷. We further find discontinuities in the relation between the mass ratio and the magnitude of the leading unstable wave-vector for both two- (2D) and three-dimensional (3D) cases. These discontinuities may indicate exotic quantum phase transitions between crys-

talline phases with different structures. The ground-state phase diagrams are concluded and partially conjectured for both 2D and 3D. A simple scaling relation generalizes these results to all mass scales.

II. METHODS

The system we consider here consists of positive and negative fermionic ions. They are of the same number N , equally charged with unit electron charge, and confined in a D -dimensional volume V . For convenience, we use Wigner-Seitz radius r_s , which is the radius of a sphere containing one electron, to parametrize the number density $\rho_0 = N/V$. All the quantities, operators and equations are in atomic units and subscripted by p, n for the two positively and negatively charged components respectively. The total Hamiltonian for the many-body system reads:

$$\mathcal{H}_{\text{total}} = \sum_{a=p,n} \left(- \sum_i^N \frac{\nabla_{a,i}^2}{2m_a} + \sum_{i<j}^N \frac{1}{|\mathbf{r}_i^a - \mathbf{r}_j^a|} \right) - \sum_{i,j}^N \frac{1}{|\mathbf{r}_i^p - \mathbf{r}_j^n|} \quad (1)$$

Further we will simply use $\gamma \geq 1$ to denote the mass ratio between the heavier component and the lighter one, and m^* to represent the larger mass and thus the mass scale, since reversing the signs of the charges does not affect the physics here.

The main assumption of our treatment is the neglect the quantum correlation between two components. It is equivalent to separating the wave-functions of different components, which is known as Born-Oppenheimer approximation and has been widely adopted in molecular physics studies. The approximation can at least be partially justified at large mass ratio γ , by recognizing the difference between the time scales of the two components motions. We will further discuss the effect of recovering such correlation in Sec. IV.

Then the two subsystems can be viewed independent, except for the local external potentials provided by the other, which arise from the Hartree part of the interaction between them. The two systems can thus be treated separately with DFT. In the high density (low r_s) region near the quantum limit, the plasma favors a near-uniform density distribution due to the dominance of the kinetic energy, whose strength is $\propto r_s^{-2}$ overwhelming the $\sim r_s^{-1}$ interaction. Under such circumstance, LSDA can be feasibly applied. As we will further discuss below, the reliability of LSDA, both in the sense of the accuracy of the functional as fitted from QMC results and, more importantly, as an approximation applied to our many-body Hamiltonian, is uncertain and will require further validation. Especially in the more strongly correlated regime, with larger r_s for instance, there can be a breakdown.

Assuming $\boldsymbol{\rho}^a = (\rho_\uparrow^a, \rho_\downarrow^a)$ and $\rho^a = \rho_\uparrow^a + \rho_\downarrow^a$ represent the (up-, down-) spin and the total density of component $a = p, n$, and defining $\boldsymbol{\rho} = (\boldsymbol{\rho}^p(\mathbf{r}), \boldsymbol{\rho}^n(\mathbf{r})) = (\rho_\uparrow^p, \rho_\downarrow^p, \rho_\uparrow^n, \rho_\downarrow^n)$, the total ground-state energy as a functional of these density distributions can be written as the sum of the two components' kinetic, exchange-correlation energies and the Hartree energy of the whole system^{16,17}:

$$E[\boldsymbol{\rho}] = \sum_{a=p,n} (T^a[\boldsymbol{\rho}^a] + E_{\text{xc}}^a[\boldsymbol{\rho}^a]) + E_{\text{Hartree}}[\rho^p, \rho^n], \quad (2)$$

where $T^a[\boldsymbol{\rho}^a]$ is the ground-state energy of an auxiliary non-interacting system with the same density distribution $\boldsymbol{\rho}^a$, $E_{\text{xc}}^a[\boldsymbol{\rho}^a] = \int d\mathbf{r} \rho^a \epsilon_{\text{xc}}^a(\boldsymbol{\rho}^a)$ within LSDA, and the Hartree term reads:

$$E_{\text{Hartree}}[\rho^p, \rho^n] = \frac{1}{2} \int \frac{(\rho^p(\mathbf{r}) - \rho^n(\mathbf{r}))(\rho^p(\mathbf{r}') - \rho^n(\mathbf{r}'))}{|\mathbf{r} - \mathbf{r}'|} d\mathbf{r} d\mathbf{r}', \quad (3)$$

which couples the two components of the plasma. We acquire each component's exchange-correlation energy by scaling electron's using the relation in appendix.

It is obvious that the unpolarized uniform solution $\boldsymbol{\rho}(\mathbf{r}) = \frac{1}{2}(\rho_0, \rho_0, \rho_0, \rho_0)$ is always a stationary point of this functional, since it satisfies the Kohn-Sham equations derived from the stationary condition $\delta E_0[\boldsymbol{\rho}] = 0$. At the high density limit ($r_s \rightarrow 0$), this solution is indeed stable. While it is well-known that, at low densities (large r_s), the ground state of the jellium model of electron gas ($\gamma \rightarrow \infty$) is a Wigner crystal in both two- and three-dimensional cases, explicitly breaking translation symmetry. To investigate the possible symmetry breaking point as a function of r_s , we expand the energy functional to the second-order of an arbitrary density fluctuation $\delta\boldsymbol{\rho}(\mathbf{r}) = \rho_0 \sum_{\mathbf{q}} \delta\rho_{\mathbf{q}} e^{-i2k_F\mathbf{q}\cdot\mathbf{r}}$ around the uniform solution, where k_F denotes the magnitude of the Fermi wave-vector of a non-interacting fermionic system with the same density ρ_0 , so that the wave vector \mathbf{q} is defined in units of $2k_F$.

We can then directly expand the functional to the second order and transform to momentum space. This expansion can be written into the form of a sum of 4×4 matrices $\mathcal{H}_{\mathbf{q}}$ contracting with density fluctuations $\delta\rho_{\mathbf{q}}$ over all wave vector \mathbf{q} 's:

$$\delta^2 E = \sum_{\mathbf{q}} \delta\rho_{\mathbf{q}}^\dagger \mathcal{H}_{\mathbf{q}} \delta\rho_{\mathbf{q}}$$

where

$$\mathcal{H}_{\mathbf{q}} = \frac{N\rho_0}{2} \begin{pmatrix} A + B^p + 1/\chi^p & -A \\ -A & A + B^n + 1/\chi^n \end{pmatrix} \quad (4)$$

The spin blocks read ($\alpha, \beta = \uparrow, \downarrow$):

$$A_{\alpha\beta} \equiv h = \begin{cases} \frac{\pi}{k_F^2 q^2} & D = 3 \\ \frac{\pi}{k_F q} & D = 2 \end{cases}, \quad (5)$$

$$B_{\alpha\beta}^a = \frac{\partial^2 (\rho \epsilon_{\text{xc}}^a(\rho_\uparrow, \rho_\downarrow))}{\partial \rho_\alpha \partial \rho_\beta} \Big|_{\rho = \rho_0^a}, \quad (6)$$

which represent the Hartree and exchange-correlation energy variations. We mention that the ions' exchange-correlation energy per-particle, ϵ_{xc}^a , can be acquired by applying the scaling relation on the QMC result for the electron gas. $\chi_{\alpha\beta}^a = \delta_{\alpha\beta}\chi_0^a$ where the static Lindhard function

$$\chi_0^a = \begin{cases} \frac{m_a k_F}{4\pi^2} \left(1 + \frac{1-q^2}{2q} \ln \left| \frac{1+q}{1-q} \right| \right) & D=3 \\ \frac{m_a}{2\pi} \left(1 - \Theta(q-1)\sqrt{1-1/q^2} \right) & D=2 \end{cases} \quad (7)$$

is the linear response function of the non-interacting fermionic gas⁴⁸. Its reciprocal evaluates the second variation of the kinetic energy functionals^{49,50}.

The diagonalization of \mathcal{H}_q gives two CDW modes' eigen-energy λ_{CDW}^\pm and two SDW modes' eigen-energy $\lambda_{\text{SDW}}^{a=p,n}$ on each wave vector \mathbf{q} . They are:

$$\lambda_{\text{SDW}}^a = \frac{N\rho_0}{2} (2/\chi_0^a + B_{\uparrow\uparrow}^a - B_{\uparrow\downarrow}^a), \quad (8)$$

$$\lambda_{\text{CDW}}^\pm = \frac{N\rho_0}{4} \left(u^p + u^n + 4h \pm \sqrt{16h^2 + (u^p - u^n)^2} \right), \quad (9)$$

where we define ($a = p, n$):

$$u^a \equiv 2/\chi_0^a + B_{\uparrow\uparrow}^a + B_{\uparrow\downarrow}^a. \quad (10)$$

The corresponding eigenvectors are:

$$\rho_{\text{SDW}}^{p,n} = (1, -1, 0, 0)/\sqrt{2}, (0, 0, 1, -1)/\sqrt{2}, \quad (11)$$

$$\rho_{\text{CDW}}^\pm = (v_\pm, v_\pm, 1, 1)/\sqrt{2(1+v_\pm^2)}, \quad (12)$$

where

$$v_\pm \equiv -\frac{(u^p - u^n) \pm \sqrt{16h^2 + (u^p - u^n)^2}}{4h}. \quad (13)$$

With the decrement of density, the first eigenenergy approaching zero gives a leading unstable mode towards the deformation of the unpolarized uniform state.

III. RESULTS

In our numerical calculations of CDW spectra, we found no qualitative or quantitatively significant difference of the results when using different fittings of exchange-correlation energy, for example PZ81⁵¹, PW92⁵², or SPS10⁵³. We hence adopted two recent simple forms of the exchange-correlation energy in two- and three-dimensional systems^{25,54}. In Figs. 1 and 2, we plot several typical energy spectra (normalized by total number of particles) of the lower-energy CDW mode, $e(q) \equiv \lambda_{\text{CDW}}^-(q)/N$, for different r_s and γ .

We notice that each SDW mode only involves the density modulation of only one component, since there is

no interaction concerning spins between the two components. In three-dimensional systems, $\lambda_{\text{SDW}}^{a=p,n}(q)$ is monotonically increasing, so the $q=0$ mode must be the first unstable SDW mode, which corresponds to a spontaneous polarization of the uniform a -gas. Moreover, if we define a polarization parameter $\eta \equiv \frac{\rho_\uparrow - \rho_\downarrow}{\rho_\uparrow + \rho_\downarrow}$, then $\lambda_{\text{SDW}}^{a=p,n}$ is proportional to the second derivative of the total energy of the uniform a -gas with respect to η . As shown in Fig.5 of Ref.³³, past QMC results suggest that this derivative would not be negative for the three-dimensional electron gas until r_s becomes larger than ~ 50 . The scaling relation in the appendix further puts this point to $50m_e/m_a$ for the a -gas. Such values of r_s for polarization are much larger than the critical r_s of the CDW mode analyzed below, so the unpolarized uniform plasma would first be unstable against a CDW mode and transit to a crystalline phase in our calculations. Similar argument applies in the two-dimensional case, where we again find that the CDW instability occurs earlier than the polarization point predicted by all recent studies^{14,25-27}.

Now we turn to the analysis on the CDW mode whose eigen-energy first approaches zero as increasing r_s and its corresponding wavevector q_c . It is worth noting that, due to the Kohn anomaly of the Lindhard function, the CDW spectra share a positively divergent gradient at $q=1$. Thus for certain r_s and γ a downtrend can be introduced near that point, and the spectra would show a double well structure, as shown in Figs. 1(b) and 1(c) for 3D, and Figs. 2(b) and 2(c) for 2D, where we have labeled the two local minima on both sides of $q=1$ by q_1 and q_2 . This fine structure introduces discontinuities of the leading symmetry breaking wave-vector as γ is varied. We note that this is a pure quantum effect which is related to the Fermi surface and thus the Pauli exclusion principle. Similar but finer structures in the spectra also occur when m_p is close to m_n for 3D systems, as shown in Figs. 1(d)-1(f). These sudden changes of the wavelength of the leading unstable CDW eigenmode is seen more clearly in Fig. 3(a), where we plot the wave vector length q_c of the first unstable CDW wave against the mass ratio γ . A similar plot is shown for 2D in Fig. 4(a).

To conclude these results, we plot the critical value r_s^c , which is normalized by the mass scale m^* , versus the mass ratio γ in Figs. 3(b) and 4(b) for 3D and 2D respectively. These can be viewed as phase diagrams indicating the transition line between different crystalline phases and a uniform liquid phase. The line can be divided into parts and corresponds to different intervals of leading symmetry breaking wave-vector, which may indicate exotic quantum structural phase transitions between different crystalline phases with discontinuous lattice constant. Furthermore, from Figs. 1(b) and 1(e) in 3D and Fig. 2(b) in 2D, we can see that changing r_s while fixing γ can also alter the choice of global minimum between the two local minima in the spectrum. Based on this information we can infer possible phases in the vicinity of the phase transition line, as we have indicated with the dashed lines in Figs. 3(b) and 4(b).

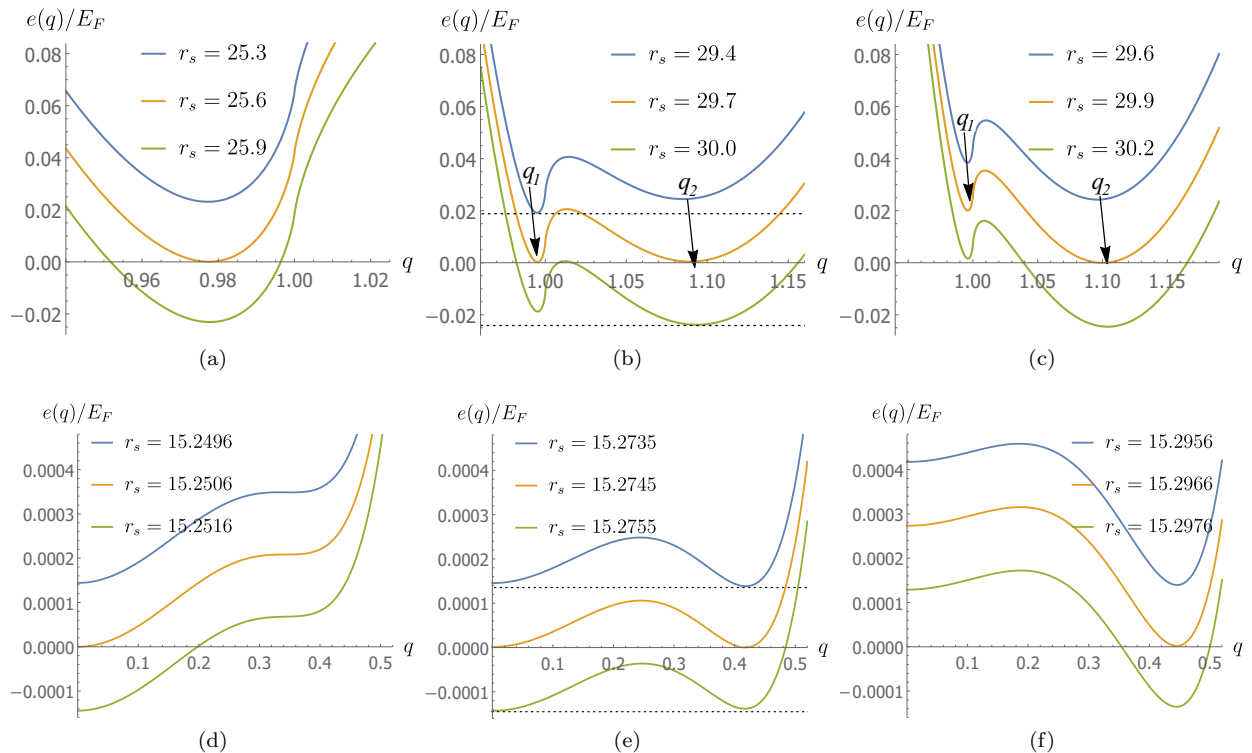


FIG. 1: The energy response in three-dimensions to the eigenmode with the smallest eigen-energy, for mass ratio $\gamma =$ (a) 24, (b) 240, (c) 2400, (d) 5.012, (e) 5.022 and (f) 5.032. The response shown is properly normalized by the total number of particles N and plotted in units of heavier particle's Fermi energy $E_F = \frac{k_F^2}{2m_*}$. The dashed lines mark the global minima of the spectra.

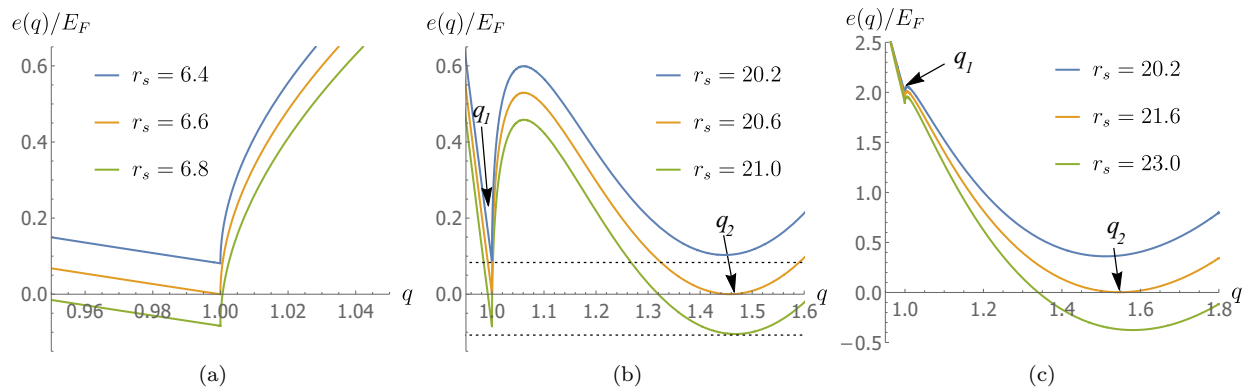


FIG. 2: The same as in Fig. 1, but for the two-dimensional case, with $\gamma =$ (a) 9.12, (b) 91.2 and (c) 912.

IV. DISCUSSIONS

We first discuss two interesting limiting cases. The first is the jellium limit as $\gamma \rightarrow \infty$ and $m^* = 1$. In this case, the heavier component becomes the electrons and the lighter one is so free that the only role it could play is a uniform background. In three dimensions, we obtain a critical Wigner radius $r_s \approx 29.9$ and a leading unstable CDW mode of wave-vector $q_c \approx 1.10$ ($2k_F$). In the two-dimensional case, the critical Wigner radius $r_s \approx 21.7$

and the corresponding wave-vector $q_c \approx 1.56$ ($2k_F$). These points are close to the earlier results acquired by similar methods^{50,55}. These symmetry breaking points occur earlier than predicted by QMC. Thus our result could be a hint for the existence of new intermediate phases for the ground state of uniform electron gas, with the discrepancy arising from the possibility that the candidate structures searched in QMC calculations so far are not yet optimal. However, it is also likely the result of the approximate treatment of the original many-body Hamil-

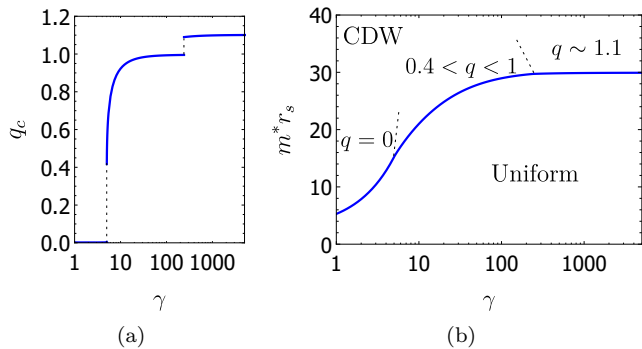


FIG. 3: (a) The first unstable CDW wave vector q_c when decreasing density for different mass ratios and (b) the phase diagram of the plasma, in three dimensions. The solid line in (b) is the exact critical r_s - γ relation, normalized by the mass scale m^* . The dashed lines are conjectured from the r_s -dependence of the energy spectra.

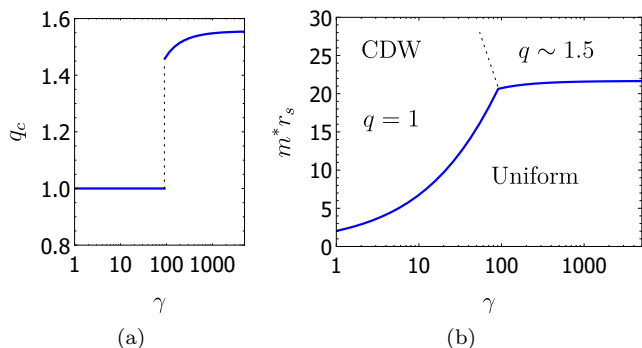


FIG. 4: The same as in Fig. 3, but for 2D.

tonian by a density-functional under LSDA, especially since this is in the regime of large r_s with strong correlation effects. Our predicted symmetry-breaking points are later than those from HF. This is also reasonable since HF will consistently overestimate the trend of (especially magnetic) inhomogeneity.

A closely related case is hydrogen, with $\gamma = m^* \approx 1837$. Our results suggest the onset of CDW at a tiny $r_s \sim 0.016$ (a.u.). (We should note that at such high densities, relativistic effects are important, which are not accounted for in our theory.) This indeed corresponds to a much higher density than the regime where previous more detailed calculations^{56–58} have identified atomic orders. Our result may shed light on the possibility of quantum solid phase in hydrogen at an ultra high density which is far beyond reach of today’s experiment.

The second case is the $1 \leq \gamma \leq 5.022$ region in 3D, where the leading unstable wave-vector is 0. Near the critical point, the $q \rightarrow 0$ modes of negative energies have $\rho_{\text{CDW}}^- \approx (1, 1, 1, 1)/2$, which indicates that the system favors to bodily move and the macro fluctuations induced by the long-wavelength density waves would force the system to be no longer confined by the volume V but

self-confined to a denser state by cohesive force. In other words, phase separation occurs in this regime, which also implies the nonexistence of quantum crystal when the masses of the two components are close. Similar results have also been reported at finite temperatures^{5,6,59}.

As mentioned, it is a major approximation to treat the p - n interaction only by the Hartree approximation. It is reasonable to consider whether adding back the p - n correlation effect would change our results. This of course can not be definitely answered without a better treatment. However a few hints are available from formal considerations. For example we could consider adding back a p - n correlation functional E_c^{p-n} in Eq. 2 like in a previous DFT study on the two component system⁶⁰. This term would modify the behavior of the mediating electronic force at second order of expansion, but would not eliminate the Kohn anomalies in the spectra, thus not the double well structures near $q = 1$ for intermediate mass ratios. Moreover, it can be easily checked that the critical q_c remains unchanged at the two limiting cases, $\gamma \rightarrow 1$ and ∞ . This would imply that, as γ varies from 1 to ∞ , q_c still must go through a discontinuity around 1. Thus we conclude that at least the correlation effect would not qualitatively affect the existence of the discontinuity near $2k_F$ in the relation between critical wave-vector and mass ratio. We remark that, since the anomalous discontinuity is rooted from the nature of fermionic response functions and varying mass ratio is equivalently tuning the strength of Coulomb screening, then adjusting other parameters that plays the same role might also introduce similar phenomena in different system settings.

There are indeed regimes where this framework breaks down. For example when $\gamma = 1$, QMC calculations indicate that Bose condensation of excitonic molecules occurs at rather small r_s ^{12,61}. In these situations, we believe the following generalization of our approach would lead to significant improvements while adding little additional complexity. We could consider a Kohn-Sham variational wave function in the form of a product of projected BCS wave functions (Antisymmetrized Germinal Powers, AGPs), each of which describes a pairing state between the two species (for example, one for pairing between p_\uparrow and n_\downarrow , while the other for p_\downarrow and n_\uparrow). The computational manipulations necessary for using such a wave function with the Kohn-Sham plus p - n Hartree Hamiltonian are readily available (see e.g., Ref.⁶²).

It is worth noting that, if the energy functional remains valid at small density variation, the exotic phase transition around $\sim 2k_F$ could also be identified by probing different energy dispersion relations of the phonon-like Goldstone mode. Expanding a spatially slowly varying phase $u(\mathbf{x})$ of the condensed amplitude $\rho_{\mathbf{q}_c} = |\rho_{\mathbf{q}_c}| e^{-iu(\mathbf{x})}$, we find that the energy dispersion of the $u_{\mathbf{p}}$ mode is proportional to that of the $\rho_{\mathbf{q}_c+\mathbf{p}}$ mode. Thus the quantitative (for 3D) or qualitative (for 2D) difference in the appearance of the energy dispersions around two local minima, shown in Figs. 1(b) for 3D and 2(b) for 2D,

may possibly be observed by spectroscopic experiments. This is especially interesting for the case of the minimum lying exactly at $2k_F$ in the 2D system. The sharp turning of the CDW mode dispersion indicates a linear (quadratic) dispersion of the Goldstone mode along (perpendicular to) the symmetry breaking direction, which is different from traditional theory of the elastic behavior for short-range correlated smectic liquid crystals⁶³.

Lastly, we remark that our results suggest the possible existence of “quantum crystals.” Since tuning parameters such as mass ratio can change the characteristic length scale in the system, lattices at intermediate density can possess non-integer numbers of particles per unit cell, which is never the case in classical crystals. This is an interesting direction for further investigations, for example with more explicit calculations.

V. CONCLUSION

In summary, we have proposed a quantum model for a two-component fermionic plasma and a theoretical approach for treating it. We formulate an approximate numerical solution based on the theory of DFT using LSDA,

and obtain the critical values of density and wave-vector where an instability of the uniform state against a CDW occurs. When the mass ratio is varied from 1 to $+\infty$, we identify several distinct ranges of critical CDW wave-vector lengths in both the two- and three-dimensional cases, which may indicate different structures of quantum crystalline phases. Zero-temperature phase diagrams are provided. A simple scaling relation is given which allows the results to be generalized to any mass scale. With the framework presented in this work, one can expect that higher order perturbative expansions of the functional would support the analysis on possible instabilities towards more exotic density ordering phases (e.g. non-collinear magnetism).

Acknowledgement

We thank Steven A. Kivelson, David M. Ceperley, Markus Holzmann, and Xin-Zheng Li for helpful discussions. S.Z. acknowledges support from NSF DMR-1409510. The Flatiron Institute is a division of the Simons Foundation.

-
- * Electronic address: szhang@flatironinstitute.org
 † Electronic address: daix@ust.hk
- ¹ C. Pierleoni and D. Ceperley, in *Computer Simulations in Condensed Matter Systems: From Materials to Chemical Biology Volume 1* (Springer Berlin Heidelberg, Berlin, Heidelberg, 2006) pp. 641–683.
 - ² M. A. Morales, C. Pierleoni, and D. M. Ceperley, *Physical Review E* **81**, 021202 (2010).
 - ³ K.-d. Oh and P. A. Deymier, *Physical Review Letters* **81**, 3104 (1998).
 - ⁴ B. Militzer and D. M. Ceperley, *Physical Review E* **63**, 066404 (2001).
 - ⁵ V. Filinov, M. Bonitz, P. Levashov, V. Fortov, W. Ebeling, and M. Schlanges, *Contributions to Plasma Physics* **43**, 290 (2003).
 - ⁶ V. S. Filinov, M. Bonitz, P. Levashov, V. E. Fortov, W. Ebeling, M. Schlanges, and S. W. Koch, *Journal of Physics A: Mathematical and General* **36**, 6069 (2003).
 - ⁷ S. V. Shevkunov, *Journal of Experimental and Theoretical Physics* **100**, 617 (2005).
 - ⁸ W. Ebeling, V. E. Fortov, and V. Filinov, *Quantum Statistics of Dense Gases and Nonideal Plasmas*, Springer Series in Plasma Science and Technology (Springer International Publishing, Cham, 2017).
 - ⁹ W. F. Brinkman and T. M. Rice, *Phys. Rev. B* **7**, 1508 (1973).
 - ¹⁰ O. Hildebrand, E. O. Goebel, K. M. Romanek, H. Weber, and G. Mahler, *Physical Review B* **17**, 4775 (1978).
 - ¹¹ M. Saba, M. Cadelano, D. Marongiu, F. Chen, V. Sarritzu, N. Sestu, C. Figus, M. Aresti, R. Piras, A. Geddo Lehmann, C. Cannas, A. Musinu, F. Quochi, A. Mura, and G. Bongiovanni, *Nature Communications* **5**, 5049 (2014).
 - ¹² X. Zhu, M. S. Hybertsen, and P. B. Littlewood, *Phys. Rev. B* **54**, 13575 (1996).
 - ¹³ M. Tuckerman and D. Ceperley, *The Journal of Chemical Physics* **148**, 102001 (2018), <https://aip.scitation.org/doi/pdf/10.1063/1.5026714>
 - ¹⁴ P.-F. Loos and P. M. W. Gill, *Wiley Interdisciplinary Reviews: Computational Molecular Science* **6**, 410 (2016).
 - ¹⁵ G. Giuliani and G. Vignale, *Quantum Theory of the Electron Liquid* (Cambridge University Press, Cambridge, 2005).
 - ¹⁶ W. Kohn and L. J. Sham, *Physical Review* **137**, A1697 (1965).
 - ¹⁷ W. Kohn and L. J. Sham, *Physical Review* **140**, A1133 (1965).
 - ¹⁸ R. M. Martin, *Electronic Structure: Basic Theory and Practical Methods* (Cambridge University Press, 2004).
 - ¹⁹ E. Wigner, *Physical Review* **46**, 1002 (1934).
 - ²⁰ Y. P. Monarkha and V. E. Syvokon, *Low Temperature Physics* **38**, 1067 (2012).
 - ²¹ G. Senatore and G. Pastore, *Phys. Rev. Lett.* **64**, 303 (1990).
 - ²² N. Choudhury and S. K. Ghosh, *Phys. Rev. B* **51**, 2588 (1995).
 - ²³ D. M. Ceperley and B. J. Alder, *Physical Review Letters* **45**, 566 (1980).
 - ²⁴ B. Tanatar and D. M. Ceperley, *Physical Review B* **39**, 5005 (1989).
 - ²⁵ N. D. Drummond and R. J. Needs, *Physical Review Letters* **102**, 126402 (2009).
 - ²⁶ C. Attacalite, S. Moroni, P. Gori-Giorgi, and G. B. Bachelet, *Physical Review Letters* **88**, 256601 (2002).
 - ²⁷ P. Gori-Giorgi, C. Attacalite, S. Moroni, and G. B.

- Bachelet, *International Journal of Quantum Chemistry* **91**, 126 (2003).
- ²⁸ D. Ceperley, *Physical Review B* **18**, 3126 (1978).
- ²⁹ Y. Kwon, D. M. Ceperley, and R. M. Martin, *Physical Review B* **48**, 12037 (1993).
- ³⁰ G. Ortiz and P. Ballone, *Physical Review B* **50**, 1391 (1994).
- ³¹ G. Ortiz and P. Ballone, *Physical Review B* **56**, 9970 (1997).
- ³² G. Ortiz, M. Harris, and P. Ballone, *Physical Review Letters* **82**, 5317 (1999).
- ³³ F. H. Zong, C. Lin, and D. M. Ceperley, *Physical Review E* **66**, 036703 (2002).
- ³⁴ N. D. Drummond, M. D. Towler, and R. J. Needs, *Physical Review B* **70**, 235119 (2004).
- ³⁵ H. Falakshahi and X. Waintal, *Physical Review Letters* **94**, 046801 (2005).
- ³⁶ X. Waintal, *Physical Review B* **73**, 075417 (2006).
- ³⁷ B. K. Clark, M. Casula, and D. M. Ceperley, *Physical Review Letters* **103**, 055701 (2009).
- ³⁸ G. G. Spink, R. J. Needs, and N. D. Drummond, *Physical Review B* **88**, 085121 (2013).
- ³⁹ B. Bernu, F. Delyon, M. Holzmann, and L. Baguet, *Physical Review B* **84**, 115115 (2011).
- ⁴⁰ J. R. Trail, M. D. Towler, and R. J. Needs, *Physical Review B* **68**, 045107 (2003).
- ⁴¹ S. Zhang and D. M. Ceperley, *Physical Review Letters* **100**, 236404 (2008).
- ⁴² L. Baguet, F. Delyon, B. Bernu, and M. Holzmann, *Physical Review Letters* **111**, 166402 (2013).
- ⁴³ L. Baguet, F. Delyon, B. Bernu, and M. Holzmann, *Physical Review B* **90**, 165131 (2014).
- ⁴⁴ R. Méndez-Moreno, M. Ortiz, S. Orozco, and M. Moreno, *Solid State Communications* **121**, 223 (2002).
- ⁴⁵ Y. Ito, K. Okazaki, and Y. Teraoka, *Physica E: Low-dimensional Systems and Nanostructures* **22**, 148 (2004), 15th International Conference on Electronic Properties of Two-Dimensional Systems (EP2DS-15).
- ⁴⁶ Y. Ito and Y. Teraoka, *Journal of Magnetism and Magnetic Materials* **310**, 1073 (2007), proceedings of the 17th International Conference on Magnetism.
- ⁴⁷ E. Fradkin, in *Modern Theories of Many-Particle Systems in Condensed Matter Physics*, Lecture Notes in Physics, Vol. 843, edited by D. C. Cabra, A. Honecker, and P. Pujol (Springer Berlin Heidelberg, Berlin, Heidelberg, 2012).
- ⁴⁸ B. Mihaila, (2011), arXiv:1111.5337.
- ⁴⁹ P. Hohenberg and W. Kohn, *Physical Review* **136**, B864 (1964).
- ⁵⁰ J. P. Perdew and T. Datta, *physica status solidi (b)* **102**, 283 (1980).
- ⁵¹ J. P. Perdew and A. Zunger, *Physical Review B* **23**, 5048 (1981).
- ⁵² J. P. Perdew and Y. Wang, *Physical Review B* **45**, 13244 (1992).
- ⁵³ J. Sun, J. P. Perdew, and M. Seidl, *Physical Review B* **81**, 085123 (2010).
- ⁵⁴ T. Chachiyo, *The Journal of Chemical Physics* **145**, 021101 (2016).
- ⁵⁵ L. M. Sander, J. H. Rose, and H. B. Shore, *Physical Review B* **21**, 2739 (1980).
- ⁵⁶ J. Chen, X.-Z. Li, Q. Zhang, M. I. Probert, C. J. Pickard, R. J. Needs, A. Michaelides, and E. Wang, *Nature communications* **4**, 2064 (2013).
- ⁵⁷ J. M. McMahon, M. A. Morales, C. Pierleoni, and D. M. Ceperley, *Rev. Mod. Phys.* **84**, 1607 (2012).
- ⁵⁸ D. Ceperley, in *NATO Advanced Science Institutes (ASI) Series B*, NATO Advanced Science Institutes (ASI) Series B, Vol. 186, edited by A. Polian, P. Loubeyre, and N. Boccaro (1989) p. 477.
- ⁵⁹ M. Bonitz, V. S. Filinov, V. E. Fortov, P. R. Levashov, and H. Fehske, *Physical Review Letters* **95**, 235006 (2005).
- ⁶⁰ E. Boroński and R. M. Nieminen, *Phys. Rev. B* **34**, 3820 (1986).
- ⁶¹ J. Shumway and D. Ceperley, *Le Journal de Physique IV* **10**, Pr5 (2000).
- ⁶² H. Shi and S. Zhang, *Phys. Rev. B* **95**, 045144 (2017).
- ⁶³ P. M. Chaikin and T. C. Lubensky, “Generalized elasticity,” in *Principles of Condensed Matter Physics* (Cambridge University Press, 1995) p. 288352.
- ⁶⁴ K. Kärkkäinen, M. Koskinen, S. M. Reimann, and M. Manninen, *Physical Review B* **68**, 205322 (2003).
- ⁶⁵ A. Altland and B. Simons, *Condensed Matter Field Theory* (Cambridge University Press, Cambridge, 2006).

Appendix A: A Scaling Relation for Different Mass Scales

We have the Hamiltonian

$$\hat{H} = - \sum_i \frac{1}{2m_i} \nabla_i^2 + \sum_{i<j} \frac{q_i q_j}{|\mathbf{r}_i - \mathbf{r}_j|} \quad (\text{A1})$$

for a system confined in a given D -dimensional volume V consisting of several components of N charged fermions. A Wigner radius can still be defined, as in the main text, to parametrize the number density $\rho_0 = N/V$. Let $\boldsymbol{\xi} = (\mathbf{r}_1, \mathbf{r}_2, \dots, \mathbf{r}_N)$ and suppose that $\psi(\boldsymbol{\xi})$ is an eigenstate of such a system, which satisfies:

$$\hat{H}\psi(\boldsymbol{\xi}) = E\psi(\boldsymbol{\xi}) \quad (\text{A2})$$

Now we perform a coordinate transformation, by replacing all \mathbf{r}_i by $k\bar{\mathbf{r}}_i$ in the equation above:

$$\left(- \sum_i \frac{1}{2m_i k^2} \nabla_i^2 + \sum_{i<j} \frac{q_i q_j}{k|\bar{\mathbf{r}}_i - \bar{\mathbf{r}}_j|} \right) \psi(k\bar{\boldsymbol{\xi}}) = E\psi(k\bar{\boldsymbol{\xi}}). \quad (\text{A3})$$

Defining a compressed wave-function $\bar{\psi}(\bar{\boldsymbol{\xi}}) \equiv \psi(k\boldsymbol{\xi})$ in the space $\bar{V} = V/k^D$, and rearranging the equation into the form:

$$\left(- \sum_i \frac{1}{2km_i} \bar{\nabla}_i^2 + \sum_{i<j} \frac{q_i q_j}{|\bar{\mathbf{r}}_i - \bar{\mathbf{r}}_j|} \right) \bar{\psi}(\bar{\boldsymbol{\xi}}) = kE \cdot \bar{\psi}(\bar{\boldsymbol{\xi}}), \quad (\text{A4})$$

we can immediately see that the operator on the left-hand side is the Hamiltonian of another system with each component having k times larger mass, i.e. $\bar{m}_i = km_i$. Hence we know that $\bar{E} \equiv kE$ is an eigen-energy and $\bar{\psi}(\bar{\boldsymbol{\xi}})$ is the corresponding eigenstate of the new system confined in the volume $\bar{V} = V/k^D$ with $\bar{r}_s = r_s/k$. We mention that

a similar argument has been proposed in ⁶⁴ and that these relations can be thought of as applications of more general scaling theory in the renormalization group ⁶⁵.

In particular, this system can be a two-component plasma and the eigenstate can be the ground state. Thus the ground-state energy and density distributions we have obtained in this paper can be easily generalize to all combinations of the masses, by scaling the whole system.

For the case of one-component electron system, the scaling relations of the interacting and non-interacting uniform ground-states read:

$$\begin{aligned} E_0(r_s) &= k\bar{E}_0(kr_s) \\ T_0(r_s) &= k\bar{T}_0(kr_s) \end{aligned}$$

where T_0 and \bar{T}_0 are the kinetic energies within the Fermi spheres and E_0 and \bar{E}_0 are the uniform ground-state energies of two jellium systems with mass m_e and km_e . Recalling the definition of exchange-correlation energy of uniform electron gas, $\epsilon_{xc} = (E_0 - T_0)/N$, we acquire the exchange-correlation energy $\bar{\epsilon}_{xc}(\bar{r}_s) = k\epsilon_{xc}(kr_s)$ for particles with mass km_e and equal charge. We note that this scaling relation holds for any polarization since the scaling operation does not change the ratio between up- and down-spin particles.